Cell Host & Microbe
Article

Shigella Targets Epithelial Tricellular Junctions and Uses a Noncanonical Clathrin-Dependent Endocytic Pathway to Spread Between Cells

Makoto Fukumatsu,[1] Michinaga Ogawa,[3] Satoko Arakawa,[4] Masato Suzuki,[3] Kazuhisa Nakayama,[5] Shigeomi Shimizu,[4] Minsoo Kim,[6] Hitomi Mimuro,[2] and Chihiro Sasakawa[1,3,7,*]
[1]Department of Infectious Disease Control, International Research Center for Infectious Disease
[2]Division of Bacteriology, Department of Infectious Disease Control, International Research Center for Infectious Disease
[3]Division of Bacterial infection, Department of Microbiology and Immunology, Institute of Medical Science
University of Tokyo, 4-6-1 Shirokanedai, Minato-ku, Tokyo 108-8639, Japan
[4]Department of Pathological Cell Biology, Medical Research Institute, Tokyo Medical and Dental University, 1-5-45 Yushima, Bunkyo-ku, Tokyo 113-8510, Japan
[5]Department of Physiological Chemistry, Graduate School of Pharmaceutical Sciences, Kyoto University, 46-29 Yoshida-Shimoadachi-cho, Sakyo-ku, Kyoto 606-8501, Japan
[6]Division of Bacterial Infection Biology, Institute of Medical Science, University of Tokyo, Minato-ku, Tokyo 108-8639, Japan
[7]Nippon Institute for Biological Science, 9-2221-1 Shinmachi, Ome, Tokyo 198-0024, Japan
*Correspondence: sasakawa@ims.u-tokyo.ac.jp
DOI 10.1016/j.chom.2012.03.001

SUMMARY

Bacteria move between cells in the epithelium using a sequential pseudopodium-mediated process but the underlying mechanisms remain unclear. We show that during cell-to-cell movement, *Shigella*-containing pseudopodia target epithelial tricellular junctions, the contact point where three epithelial cells meet. The bacteria-containing pseudopodia were engulfed by neighboring cells only in the presence of tricellulin, a protein essential for tricellular junction integrity. *Shigella* cell-to-cell spread, but not pseudopodium protrusion, also depended on phosphoinositide 3-kinase, clathrin, Epsin-1, and Dynamin-2, which localized beneath the plasma membrane of the engulfing cell. Depleting tricellulin, Epsin-1, clathrin, or Dynamin-2 expression reduced *Shigella* cell-to-cell spread, whereas AP-2, Dab2, and Eps15 were not critical for this process. Our findings highlight a mechanism for *Shigella* dissemination into neighboring cells via targeting of tricellular junctions and a noncanonical clathrin-dependent endocytic pathway.

INTRODUCTION

Bacterial pathogens that invade the cytosol of nonphagocytic host cells often rely on actin polymerization at one pole of a bacterium to move within and between host cells during infection. *Shigella* and *Listeria monocytogenes*, for example, can spread between epithelial cells, a process that consists of at least three distinct stages (Tilney and Portnoy, 1989; Cossart and Sansonetti, 2004). First, a motile bacterium attaches to and pushes on the host plasma membrane, resulting in protrusion of a pseudopodium. Second, a neighboring cell engulfs the protruding pseudopodium. Finally, the two plasma membranes surrounding the engulfed bacteria are lysed, allowing the bacterium to move into the cytoplasm of the neighboring cell. During this process, *Shigella* expresses VirG (IcsA) asymmetrically over the bacterial surface as they multiply within the epithelial cells. VirG protein accumulates at one pole of the bacterium and induces actin polymerization via recruitment of N-WASP and Arp2/3 complexes; this process provides *Shigella* with the propulsive force required to move within or between cells (Ogawa et al., 2008).

Intercellular adhesion of epithelial cells is mediated by cell-cell junctions, which are composed of tight junctions, adherence junctions, and desmosomes. Tight and adherence junctions form apical junctional complexes, consisting of several transmembrane and cytosolic components. The apical junctional complex plays important roles in modulating paracellular permeability, remodeling cell-cell contacts, and sustaining a barrier to prevent the passage of macromolecules and microbes (Steed et al., 2010). Epithelial monolayers, such as the intestinal epithelium, are composed of cells that are arranged in a grid or honeycomb-like pattern. Cell-cell contact occurs via two types of tight junctions: bicellular tight junctions (bTJs) and tricellular (multicellular) tight junctions (tTJs), where two cells and three/four cells connect, respectively. tTJs contain tricellulin, which localizes to the apical site of tTJs (Ikenouchi et al., 2005), forms barriers to macromolecules, and maintains the integrity of epithelial cells (Ikenouchi et al., 2005, 2008; Krug et al., 2009). Tricellulin also localizes at bTJs, albeit to a less extent than at tTJs, and is somewhat functionally redundant with occludins (Ikenouchi et al., 2005, 2008; Westphal et al., 2010). The barrier function and structure of tight junctions are known to be dynamic under the physiologic and pathophysiologic conditions (Steed et al., 2010). The intestinal epithelium undergoes rapid turnover, an essential homeostatic mechanism characterized by cell shedding

and transient formation of local gaps that are immediately sealed by neighboring cells (Koch and Nusrat, 2009; Pentecost et al., 2010). Endocytosis and recycling of tight junction proteins are required to remodel cell-cell junctions; these processes can be induced in response to inflammation, which causes recycling of proteins localized at the apical junctional complex and is involved in the formation and sorting of vesicles between the junctional and cytosolic pools. Thus, the plasma membrane around tight and adherence junctions likely undergoes significant remodeling (Ivanov et al., 2005; Steed et al., 2010; Utech et al., 2010).

Such cell-cell junctions as tight and adherence junctions likely play structurally and functionally important roles during bacterial spreading between epithelial cells. An early study with a mouse fibroblast cell line indicated that E-cadherin is involved in *Shigella* cell-cell spreading (Sansonetti et al., 1994). A later study showed that connexin proteins, such as connexin 26, play important roles in *Shigella* invasion and movement into adjacent epithelial cells (Tran Van Nhieu et al., 2003). Tran Van Nhieu et al. demonstrated that *Shigella* infection induced transient peaks in the intracellular calcium concentration, which opened connexin 26 hemichannels and allowed the release of ATP into the medium. The authors showed that ATP promoted calcium influx, which in turn promoted bacterial invasion and cell-cell spreading. These studies suggested that epithelial cell-cell contact and intercellular signaling are important for bacterial spreading.

Invasive pathogens are internalized by epithelial cells via two mechanisms: zippering and triggering (Cossart and Sansonetti, 2004). Pathogens that take advantage of zippering, including *L. monocytogenes*, *Yersinia pseudotuberculosis*, *Staphylococcus aureus*, *Streptococcus pyogenes*, *Chlamydia trachomatis*, and *Candida albicans*, express ligand proteins on their surfaces that interact directly or indirectly with host cellular surface receptors and stimulate actin polymerization and membrane extension to engulf the bacteria (Pizarro-Cerdá et al., 2010). A role for the clathrin-mediated endocytosis machinery in triggering actin polymerization and internalization of pathogens is increasingly recognized (Cureton et al., 2010; Collins et al., 2011). The formation of endocytic vesicles during clathrin-dependent endocytosis occurs via four steps: (i) assembly of the clathrin coat at the plasma membrane, (ii) invagination of the clathrin-coated pit, (iii) pinching off the neck to form an endocytic vesicle, and (iv) inward movement of the vesicle (Merrifield et al., 2005; Ferguson et al., 2009; Collins et al., 2011).

In the present study, we examined the molecular basis of *Shigella* cell-cell spreading, a critical process in the infection of intestinal epithelium by this bacterium. Our results show that *Shigella* translocates between epithelial cells primarily at tTJ cell-cell contact points, where three epithelial cells meet. At these positions, bacteria-containing pseudopodia were engulfed by neighboring cells via a noncanonical clathrin-mediated endocytic pathway.

RESULTS

Shigella Spreading between Epithelial Cells at tTJs

We used time-lapse imaging to characterize the route by which *Shigella* spreads between epithelial cells; motile bacteria were monitored from the onset of bacteria-induced membrane protrusion until spreading into an adjacent cell. To allow assessment of bacteria-containing pseudopodia, thin MK2 cells were used. When MK2 cell monolayers were infected with *Shigella*, only 20% of the bacteria spread via bTJs, whereas 80% moved into adjacent cells via tTJs (Figure 1A and Movie S1). Similar results were observed for *Shigella* spreading in other epithelial cell lines, including Caco-2, MDCK, AGS, and HeLa cells. Electron microscopic analysis confirmed that *Shigella*-containing pseudopodia frequently protruded from tTJs and were engulfed by neighboring epithelial cells (Figure 1B). tTJs, however, were not the predominant spreading route when epithelial cell monolayers were infected with *Listeria monocytogenes* (Figure 1A).

Tricellulin Is Required for *Shigella* Cell-Cell Spreading

Tricellulin is essential for tTJ and bTJ integrity (Ikenouchi et al., 2005). Therefore, we examined whether tricellulin contributes to *Shigella* cell-cell spreading by knocking down tricellulin expression in monolayers of MDCK cells and examining plaque formation as a marker of intercellular *Shigella* movement. Short hairpin RNA (shRNA)-mediated knockdown of tricellulin expression markedly reduced plaque diameters in the cell monolayer compared with control samples (Figures 1C and S1A). Importantly, knocking down tricellulin expression in MDCK cells halved the percentage of *Shigella*-containing pseudopodia that protruded from tTJs compared with control samples (Figure 1D). As reported previously (Ikenouchi et al., 2005, 2008), knockdown of tricellulin expression disrupted tTJs and colocalization of occludin at bTJs, whereas E-cadherin was not markedly affected (Figure S1B). We then knocked down occludin and E-cadherin expression in MDCK cell monolayers using shRNA (Figure S1A) and infected the cells with *Shigella*. Although knocking down occludin and E-cadherin expression reduced *Shigella* spreading between the cells, tricellulin expression knockdown had larger effects (Figure 1C). In fact, the numbers of *Shigella*-containing pseudopodia per epithelial cell were similar in cells with reduced tricellulin expression and control cells (4.3 ± 0.4 and 4.4 ± 0.6 pseudopodia/cell, respectively). Finally, we investigated the effects of shRNA-mediated knockdown of tricellulin expression on *L. monocytogenes* cell-cell spreading. MDCK cells stably expressing the tricellulin-specific shRNA were infected with *L. monocytogenes*. The number of infected cells or foci was not affected by knocking down tricellulin expression (Figure S1C). Together, these results clearly indicated that *Shigella* movement into neighboring epithelial cells depended on the presence of tricellulin and tTJs.

Phosphoinositide 3-Kinase Is Required for *Shigella* Cell-Cell Spreading

Tight contact between the *Shigella*-containing pseudopodium and the neighboring cell was important for efficient engulfment of the pseudopodium. Phosphoinositide (PI) 3-kinase is involved in remodeling the membrane surface, regulating membrane trafficking and signal transduction, and modulating cytoskeletal dynamics (Lindmo and Stenmark, 2006). Therefore, we investigated the potential role of PI 3-kinase in the formation of *Shigella*-containing pseudopodia in MK2 cells by introducing GFP fused to the pleckstrin homology (PH) domain of Akt (GFP-Akt-PH), which binds to phosphatidylinositol (PtdIns) (3,4,5)P_3 and PtdIns(3,4)P_2 generated by PI 3-kinase (Rong

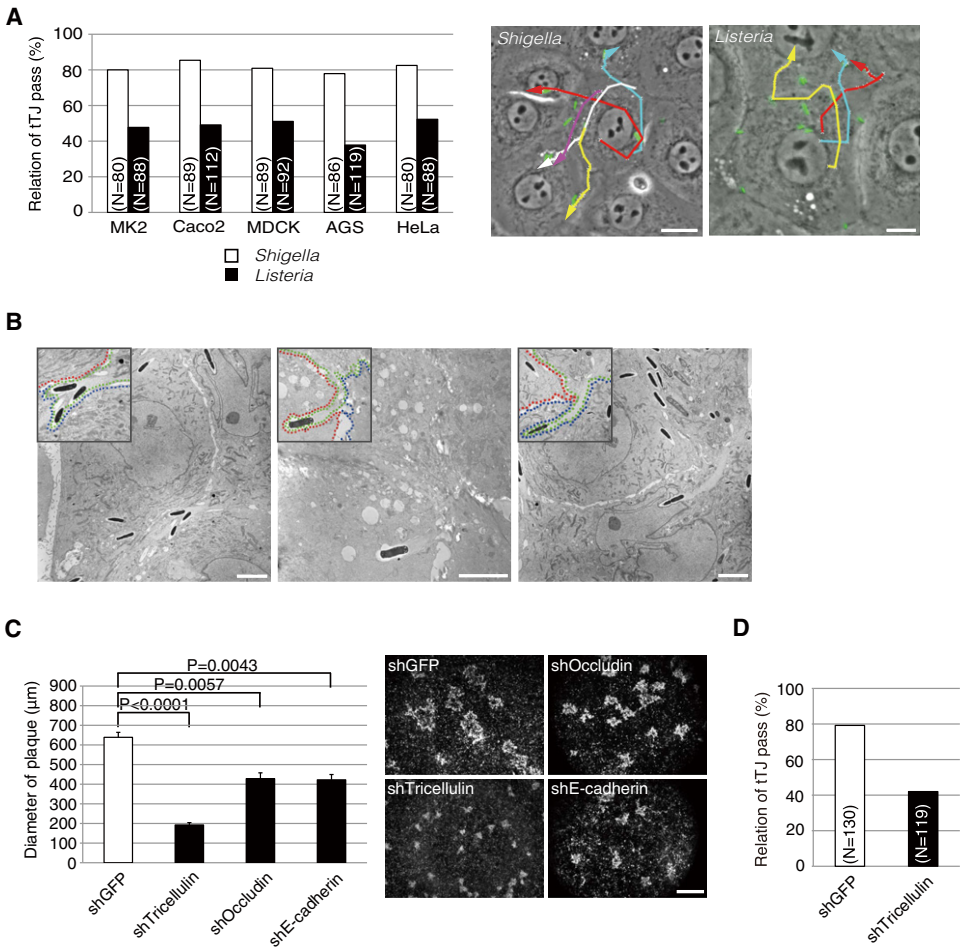

Figure 1. *Shigella* Protrude Pseudopodia at Tricellular Tight Junctions

(A) MK2 cells were infected with *Shigella* or *Listeria* for 3 hr, and the intracellular movement of each bacterium was observed. Each line indicates the trace of an intracellular *Shigella* or *Listeria*. Scale bar, 20 μm. The population of bacteria that spread via tricellular tight junctions or bicellular tight junctions was quantified. (See also Movie S1.)

(B) MK2 cells were infected with *Shigella* for 2.5 hr and then examined by electron microscopy. Scale bar, 5 μm.

(C) MDCK cells stably expressing the indicated shRNA were infected with *Shigella*. After 2 days, plaque formation was examined. Scale bar, 500 μm. The diameter of the plaques was examined. Data are the means ± SEM (>15 plaques, n = 3). (See also Figure S1.)

(D) MDCK cells stably expressing the indicated shRNA were infected with *Shigella* for 3 hr, and the ratio of bacteria that moved into adjacent cells via tricellular tight junctions or bicellular tight junctions was quantified.

et al., 2001). GFP-Akt-PH was detected around *Shigella*-containing pseudopodia that protruded from GFP-Akt-PH-negative MK2 cells into neighboring cells expressing GFP-Akt-PH. GFP-Akt-PH was observed as early as 2 min after pseudopodium engulfment (Figure 2A and Movie S2). We subsequently used Caco-2 cells (PI 3-kinase inhibitors were cytotoxic for MK2 cells) to examine the effects of the PI 3-kinase inhibitors LY294002 and wortmannin on *Shigella* cell-cell spreading. As shown in Figure 2B, bacterial intercellular spreading was reduced to less than 20% of results observed in control samples. The number of *Shigella*-containing pseudopodia per epithelial cell, however, was not affected by LY294002 (4.7 ± 0.3 versus 5.3 ± 0.5 pseudopodia/epithelial cell with and without LY294002, respectively). Giemsa staining of *Shigella*-infected Caco-2 cell monolayers confirmed that LY294002 treatment caused bacteria to accumulate at the pseudopodial tip, where they replicated but failed to spread into adjacent cells (Figures S2A and S2B). This series of experiments suggested that PI 3-kinase activity is essential in epithelial cells to trigger engulfment of *Shigella*-containing pseudopodia by the adjacent cells but not for pseudopodium formation.

Engulfment of *Shigella*-Containing Pseudopodia by Neighboring Cells Is Mediated by a Clathrin-Dependent Mechanism

There are three major endocytic membrane trafficking pathways in mammalian cells: clathrin-dependent endocytosis, caveolin-dependent endocytosis, and macropinocytosis (McMahon and Boucrot, 2011). We assessed which of these trafficking pathways is involved in *Shigella* cell-cell spreading using Caco-2 cell monolayers treated with phenylarsine oxide (PAO), methyl-β-cyclodextrin (MβCD), or 5-(N-ethyl-N-isopropyl)-amiloride

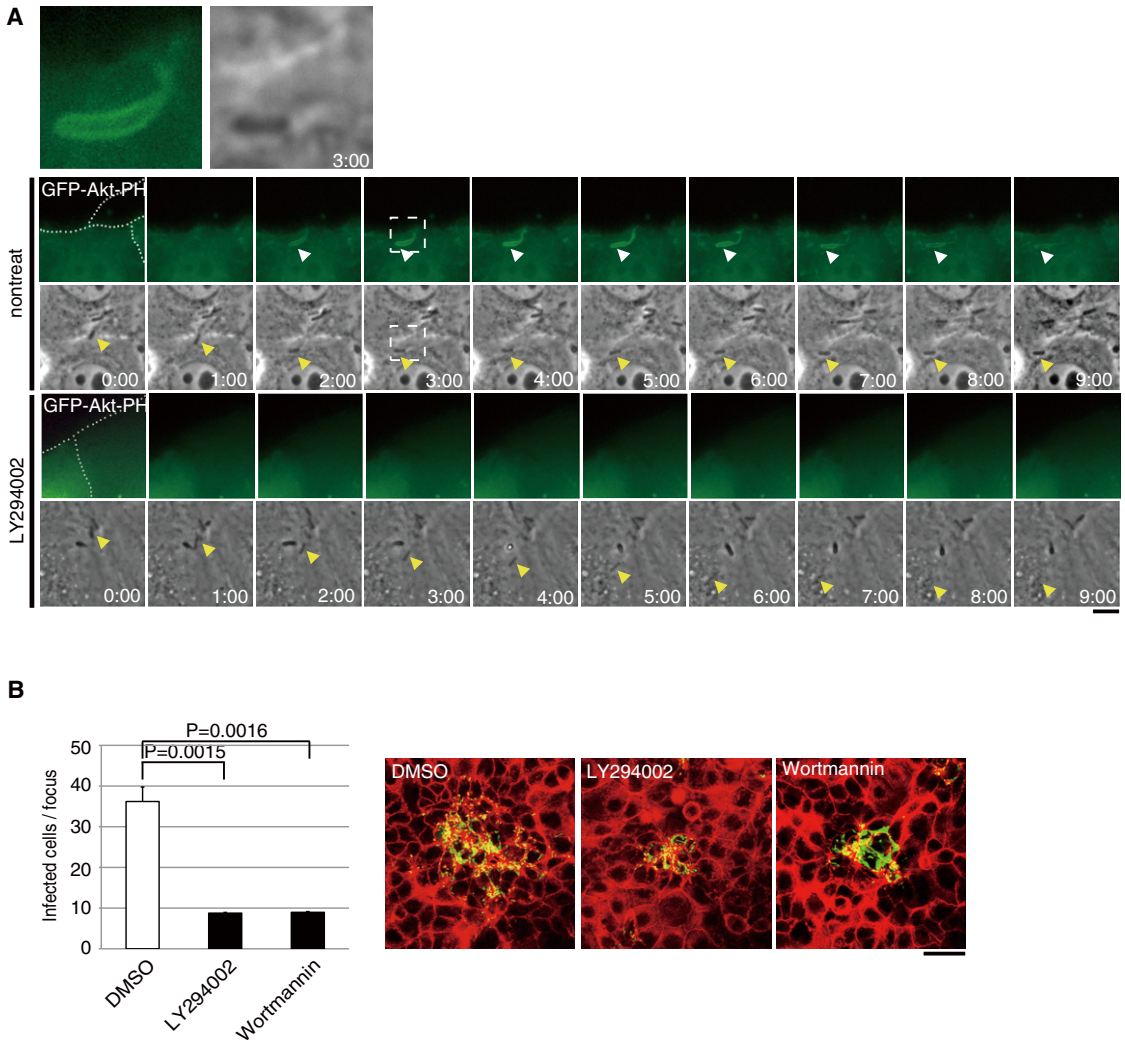

Figure 2. PI 3-Kinase Activation Is Required for *Shigella* Spreading

(A) MK2 cells expressing GFP-Akt-PH were infected with *Shigella* in the presence or absence of LY294002. After infection, images were acquired at 1 min intervals. The time after pseudopodium formation is indicated. White and yellow arrowheads indicate PtdIns(3,4,5)P_3 accumulation or *Shigella*-containing pseudopodia, respectively. Top panels are enlarged from the dashed boxes. Scale bar, 5 μm. (See also Movie S2.)

(B) Caco-2 cells were infected with GFP-expressing *Shigella* for 8 hr in the presence or absence LY294002 or wortmannin. The cells were fixed and stained with rhodamine-phalloidin. Scale bar, 50 μm. The number of cells that were infected as a result of *Shigella* spreading was counted. Data are the means ± SEM (>15 plaques, n = 3). (See also Figure S2.)

(EIPA), which respectively inhibit clathrin-dependent endocytosis, caveolin-dependent endocytosis, and macropinocytosis. Caco-2 cells treated with PAO, MβCD, or EIPA were infected with *Shigella* and examined for effects on *Shigella* cell-cell spreading. Diminished *Shigella* movement between cells was observed in Caco-2 cells treated with PAO—or to a lesser extent, in those treated with MβCD—but not those exposed to EIPA (Figure 3A). The number of *Shigella*-positive cells per foci in the monolayer decreased to 21% of results observed in untreated control samples (Figure 3A). We also investigated the effects of each inhibitor on *L. monocytogenes* cell-cell movement and found that treatment of Caco-2 monolayers with MβCD or EIPA markedly inhibited *Listeria* cell-cell movement, whereas the effects of PAO were less pronounced (Figure S3A). These results strongly suggested that *Shigella*-containing pseudopodia are taken up by neighboring cells via a clathrin-mediated trafficking pathway, which likely differs from the mechanism involved in *Listeria* cell-cell spreading.

To ensure that clathrin is involved in *Shigella* cell-cell movement, we used shRNA to knockdown clathrin expression in MDCK cells and examined *Shigella* plaque formation. As shown in Figure 3B, knocking down clathrin expression decreased the diameter of plaques to less than a third of control values. The same was true in samples with knocked down Dynamin-2 expression (Figures 3B and S3B). The number of *Shigella*-containing pseudopodia in cells with reduced clathrin or Dynamin-2 expression was 4.4 ± 0.1 or 4.2 ± 0.1 pseudopodia/cell, respectively, which was similar to results from control cells

(4.4 ± 0.2 pseudopodia/cell), suggesting that clathrin and Dynamin-2 did not substantially affect pseudopodium formation in motile *Shigella*. Furthermore, when Caco-2 cell monolayers were infected with *Shigella* and stained with antibodies specific for human clathrin or Dynamin-2, both proteins were detected around *Shigella*-containing pseudopodia (Figure 3C). MK2 cells transiently expressing clathrin-GFP or Dynamin-2-GFP that had taken up *Shigella*-containing pseudopodia were also examined using immunofluorescence microscopy. *Shigella*-containing pseudopodia protruding from clathrin-GFP-negative or Dynamin-2-GFP-negative MK2 cells into neighboring cells expressing clathrin-GFP or Dynamin-2-GFP were surrounded by GFP (Figure S3C). Time-lapse movies also showed that clathrin accumulated around long *Shigella*-containing pseudopodia that were engulfed by clathrin-GFP-expressing epithelial cells. These GFP signals were detected 30 min after infection, at which point clathrin-GFP had accumulated at the tips of the elongated pseudopodia (Figure 3D and Movie S3). In contrast, clathrin-GFP did not markedly accumulate around *Shigella*-containing pseudopodia before the 30 min time point (Figure 3D and Movie S3).

During canonical clathrin-mediated endocytosis, the clathrin coat assembles within a few minutes and Dynamin-2 induces clathrin-coated pits to pinch off from the endocytic membrane before they are translocated to early endosomes (Conibear, 2010; McMahon and Boucrot, 2011). We investigated the localization of early endosome markers relative to *Shigella*-containing pseudopodia. We infected MK2 cells expressing GFP-FYVEx2 (FYVEx2 is a domain from EEA1 that binds PtdIns(3)P; Vieira et al. [2001]) and MK2 cells expressing GFP-Rab5 cells with *Shigella*. GFP-FYVEx2 accumulated around *Shigella*-containing pseudopodia (Figure S3D). We also found that GFP-Rab5 accumulated as early as 2 min after the *Shigella*-containing pseudopodium entered a neighboring cell (Figure S3E). shRNA-mediated knockdown of Rab5 expression, however, had no effect on *Shigella* cell-cell spreading (Figure S3F), suggesting that early endosomes do not play a significant role in this process. These results indicated that a clathrin-dependent endocytotic mechanism mediates the transfer of *Shigella*-containing pseudopodia to neighboring cells.

Epsin-1 Is Essential for Engulfment of *Shigella*-Containing Pseudopodia

We further characterized clathrin-dependent endocytosis of *Shigella*-containing pseudopodia by examining the clathrin coat assembly machinery. MDCK cells were treated with shRNA to knockdown Eps15, Dab2, AP-2, or Epsin-1 expression, all of which are involved in clathrin-coated vesicle formation (McMahon and Boucrot, 2011). Examining MDCK monolayers for *Shigella* plaque formation revealed that knockdown of Epsin-1 expression reduced the average plaque size to 28% of control samples (Figures 4A and S4A), whereas subcellular localizations of tricellulin, occludin, and E-cadherin were not affected (Figure S4B). No effects were noted in this assay when AP-2, Eps15, or Dab2 expression was knocked down. An average of approximately four *Shigella*-containing pseudopodia/cell were observed in MDCK cells 3 hr post infection with or without Epsin-1 expression, implying that the adaptors do not affect pseudopodium formation during *Shigella* cell-cell spreading. Time-lapse imaging also revealed GFP-Epsin-1 around the *Shigella*-pseudopodia of infected MK2 cells after 25 min (Figure 4B and Movie S4). shRNA-mediated knockdown of Epsin-1 expression in MDCK cells resulted in less clathrin accumulation around *Shigella*-containing pseudopodium compared with control samples (Figures 4C and S4D). Reduced AP-2 expression in MDCK cells, however, did not affect clathrin accumulation around the pseudopodia (Figure S4D). These results indicated that Epsin-1 plays a role in recruiting clathrin to *Shigella*-containing pseudopodia.

We then attempted to identify the Epsin-1 domain that is required for *Shigella* cell-cell spreading. Epsin-1 consists of an epsin N-terminal homology (ENTH) domain that binds to PtdIns(4,5)P_2 and PtdIns(3,4,5)P_3 to bend the membrane (Itoh et al., 2001; Ford et al., 2002); ubiquitin-interacting motifs (UIMs) that bind polyubiquitins and ubiquitinated cargo receptors for internalization (Polo et al., 2002; Shih et al., 2002); and a C-terminal region that interacts with clathrin, Eps15, and AP-2 (Chen et al., 1998; Drake et al., 2000). We created in-frame deletions of Epsin-1 that lack the ENTH domain (ΔENTH), UIMs (ΔUIMs), or C-terminal region (ΔCOOH) (Figure 4D). We then infected MK2 cells expressing each Epsin-1 variant with *Shigella* and examined Epsin-1 along *Shigella*-containing pseudopodia taken up by neighboring cells. ΔENTH and ΔUIMs, but not ΔCOOH, failed to localize at the endocytosed pseudopodia (Figures 4D, S4C, and S4E). We also detected ubiquitin around *Shigella*-containing pseudopodia (Figure S4G). The Epsin-1 deletion mutants were then stably expressed in MDCK monolayer cells infected with *Shigella*, and plaque formation was investigated. Each of the Epsin-1 variants more than halved the size of plaques formed by *Shigella* cell-cell spreading compared with control samples (Figure 4E). Furthermore, all of the Epsin-1 deletion mutants prevented clathrin from accumulating around *Shigella*-containing pseudopodia (Figures S4C and S4F). In addition, when MK2 cells expressing clathrin-GFP or GFP-Epsin-1 and infected with *Shigella* were treated with LY294002, little clathrin or Epsin-1 accumulated around *Shigella*-containing pseudopodia (Figures 5A and 5B), demonstrating that PI 3-kinase activity was essential for recruiting Epsin-1 and clathrin to the plasma membrane where the *Shigella*-containing pseudopodia were engulfed. Together, these results show that Epsin-1 contributes to clathrin accumulation around *Shigella*-containing pseudopodia and *Shigella* cell-cell spreading.

DISCUSSION

Shigella has been used to examine various infectious mechanisms and host-pathogen interactions, although bacterial translocation between neighboring host cells was not well understood. In the present study, we investigated how bacteria-containing pseudopodia are engulfed by adjoining epithelial cells during *Shigella* cell-cell spreading. Our results show that *Shigella*-containing pseudopodia move into adjoining epithelial cells primarily at tTJs, a special epithelial junctional point at which three cells meet. Additionally, the junctional protein tricellulin plays a key role in *Shigella* cell-cell spreading. Finally, *Shigella*-containing pseudopodia are engulfed by neighboring cells via a noncanonical clathrin-mediated endocytic pathway (Figure 5C).

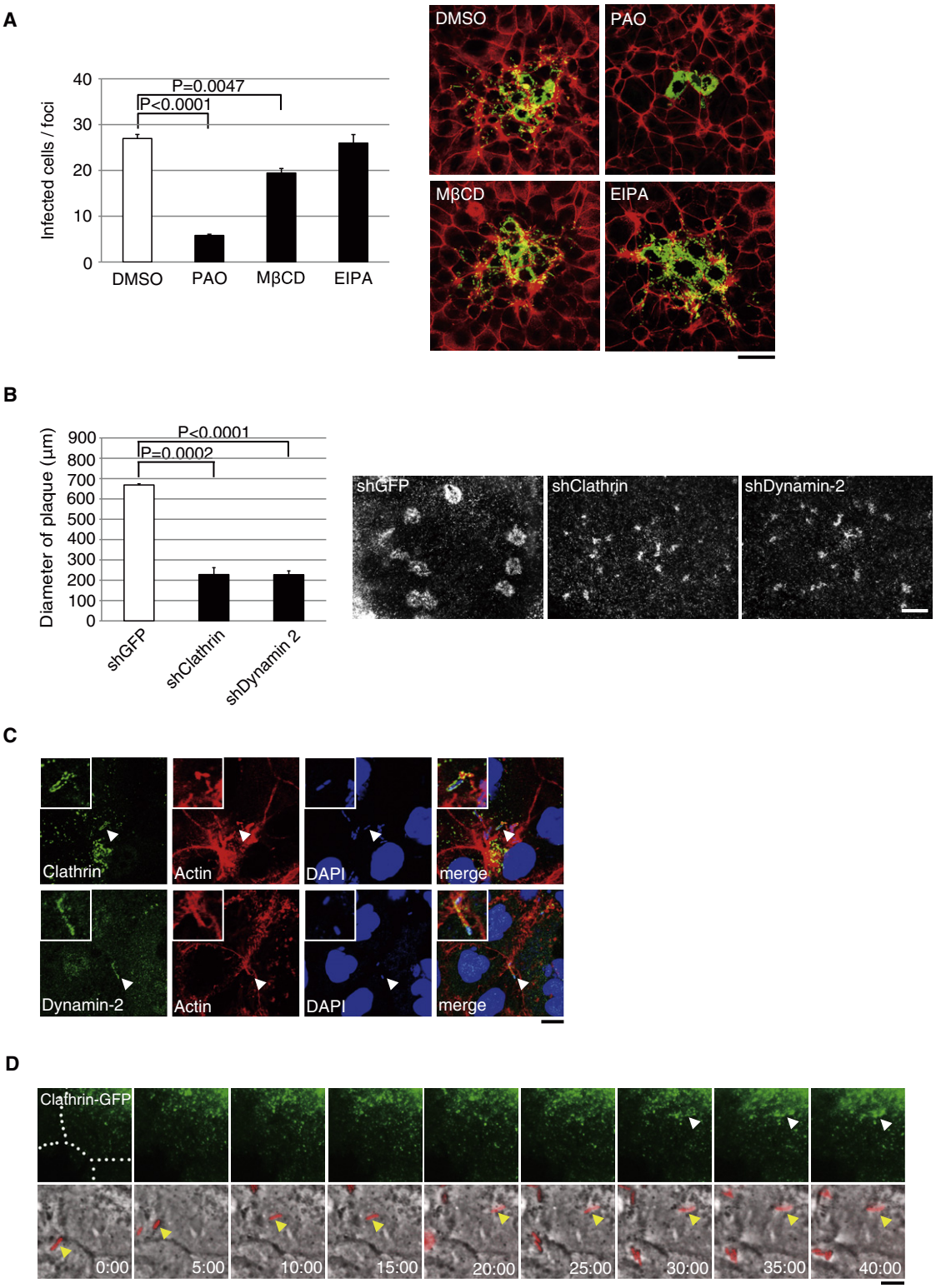

Figure 3. Clathrin-Mediated Endocytosis Is Involved in the Intercellular Spreading of *Shigella*

(A) Caco-2 cells were infected with GFP-expressing *Shigella* for 8 hr in the presence or absence of the indicated inhibitors. The cells were fixed and stained with rhodamine-phalloidin. Scale bar, 50 μm. The number of cells that were infected as a result of *Shigella* spreading was counted. Data are the means ± SEM (>15 plaques, n = 3). (See also Figure S3.)

(B) MDCK cells stably expressing the indicated shRNA were infected with *Shigella*. After 2 days, plaque formation was examined. Scale bar, 500 μm. The diameter of the plaques was measured. Data are the means ± SEM (>15 plaques, n = 3). (See also Figure S3.)

Several studies have shown that E-cadherin, myosin light chain kinase, and connexin are involved in *Shigella* intercellular movement (Sansonetti et al., 1994; Tran Van Nhieu et al., 2003; Rathman et al., 2000). Although the precise roles of these proteins have not been detailed, these studies highlight the importance of cell-cell contact and communication for bacterial spreading between epithelial cells. We found that tTJs serve as a major route for *Shigella* spreading between epithelial cells. Many studies have shown that apical junctional complexes are markedly plastic under physiologic and pathophysiologic conditions. Tight junctions are frequently remodeled under physiologic conditions and change in response to such extracellular stimuli as tumor necrosis factor and interferon-γ in inflammatory diseases (Edelblum and Turner, 2009; Shen et al., 2009); these processes are characterized by the exchange of apical junctional complex proteins from junctional and cytoplasmic pools (McMahon and Boucrot, 2011; Shen et al., 2008, 2011). In the intestinal epithelium, the plasticity of tight junctions is critically important for epithelial integrity, the intestinal barrier, and homeostasis, because bTJs and tTJs are constantly needed as dying cells are shed and the epithelium is rapidly sealed (Madara, 1990; Pentecost et al., 2006). Remodeling adhesive cell-cell contacts, including adjusting the junctional length and correctly localizing new epithelial cells, requires endocytosis and recycling of adhesion molecules (de Beco et al., 2009; Le et al., 1999; Troyanovsky et al., 2006). Therefore, the plasma membrane around tTJs may be a frequent source and destination of endocytotic vesicles (Steed et al., 2010; Utech et al., 2010), which would facilitate protrusion and engulfment of pseudopodia during *Shigella* cell-cell movement (Figures 1A and 1B).

Intriguingly, tTJs were not a preferential site of *L. monocytogenes* cell-cell spreading; 51.4% and 48.6% of *L. monocytogenes* spreading events occurred via bTJs and tTJs, respectively (Figure 1A). Interestingly, Rajabian et al. reported that the *L. monocytogenes* virulence protein internalin C (InlC) plays an important role in cell-cell spreading. InlC inhibits Tuba, which perturbs the tension between the apical junctions and facilitates protrusion of *Listeria*-containing pseudopodia from bTJs (Rajabian et al., 2009). Indeed, ectopic expression of InlC in epithelial monolayers perturbed apical junctions via interactions with Tuba, which interfered with N-WASP binding and reduced tension at bTJs (Rajabian et al., 2009). A previous study showed that Tuba is concentrated at bTJs via interactions with ZO-1 and that knocking down Tuba expression caused membrane curving and slack between cell-cell junctions (Otani et al., 2006). We, therefore, hypothesize that InlC-mediated perturbation of bTJs allows *L. monocytogenes* to protrude from pseudopodia at both bTJs and tTJs.

We identified tricellulin as an essential host factor for *Shigella* cell-cell movement. Ikenouchi et al. originally showed that suppressed tricellulin expression in epithelial cells altered the structures of tTJs and bTJs; both ends of occludin-positive bTJs thickened into a teardrop shape, suggesting that tight junction networks were disrupted in the absence of tricellulin (Ikenouchi et al., 2005). Knocking down tricellulin expression using shRNA showed similar effects on bTJ and tTJ structures and reduced *Shigella* cell-cell movement in plaque assays. When we analyzed motile *Shigella* at tTJs and their route into neighboring cells using a confocal immunofluorescence scanning microscope, we did not find any obvious patterns in the distribution of bacteria-containing pseudopodia relative to the apical surface, suggesting a lack of direct functional cooperation between tricellulin and *Shigella*-containing pseudopodium (data not shown).

In the present study, we investigated several proteins associated with clathrin-coated vesicle formation, including PI 3-kinase, Eps15, Dab2, AP-2, Epsin-1, clathrin, and Dynamin-2. Overall, our results suggest that internalization of *Shigella*-containing pseudopodia by neighboring cells is mediated by a noncanonical clathrin-mediated endocytic pathway, which depends on clathrin, Epsin-1, and Dynamin-2. Live imaging revealed that clathrin and Epsin-1 accumulated beneath the membranes of *Shigella*-containing pseudopodia 30 min after the pseudopodia were engulfed by adjacent cells (Figures 3D and 4B). We also detected GFP-Akt-PH around the endocytosed membrane as early as 2 min after internalization (Figure 2A). Moreover, PI 3-kinase inhibitors greatly diminished *Shigella* cell-cell spreading. These results together suggested that PI 3-kinase and subsequent accumulation of clathrin and Epsin-1 beneath the plasma membrane are essential for uptake of bacteria-containing pseudopodium. Of note, although AP-2 has been identified as a cargo-specific adaptor that is essential for clathrin-mediated endocytosis (McMahon and Boucrot, 2011), *Shigella*-containing pseudopodia were engulfed in the absence of AP-2 in our experiments (Figure 4A). Although trace amounts of AP-2 in shRNA-treated cells may have contributed to pseudopodium endocytosis (Figure S4A), several studies have demonstrated clathrin-mediated endocytosis in AP-2-depleted cells (Conner et al., 2003; Motley et al., 2003; Veiga and Cossart, 2005), suggesting *Shigella*-containing pseudopodia are taken up by neighboring cells in an AP-2-independent, clathrin-dependent endocytic pathway.

Among clathrin-mediated endocytosis adaptor proteins, we identified Epsin-1 as essential for internalization of *Shigella*-containing pseudopodia into neighboring cells via a clathrin-mediated mechanism. Epsin-1 is a ENTH domain-containing, membrane-bending protein and a cargo-specific adaptor for monoubiquitinated receptors (McMahon and Boucrot, 2011). Epsin-1 contains motifs that interact directly with clathrin, AP-2, and Eps15; an N-terminal ENTH domain that binds the phospholipid PtIns(4, 5)P_2; and UIMs that interact with ubiquitin and monoubiquitinated receptors. Interestingly, Epsin-1 was identified as a cargo-specific adaptor for influenza virus entry via clathrin-mediated endocytosis (Chen and Zhuang, 2008). Like our results with *Shigella*, siRNA-mediated knock down of Epsin-1 expression greatly inhibited viral entry (Chen and Zhuang, 2008). On the other hand, knocking down Epsin-1

(C) Caco-2 cells were infected with *Shigella* for 2.5 hr, fixed, and then stained with rhodamine-phalloidin (actin, red), DAPI (DNA, blue), and antibodies against the clathrin heavy chain or Dynamin-2 (green). Scale bar, 20 μm.

(D) MK2 cells were transfected with clathrin-GFP and then infected with *Shigella*. Images were acquired at 1 min intervals after infection. The time after pseudopodium formation is indicated. White and yellow arrowheads indicate clathrin accumulation and *Shigella*-containing pseudopodia, respectively. Scale bar, 5 μm. (See also Movie S3.)

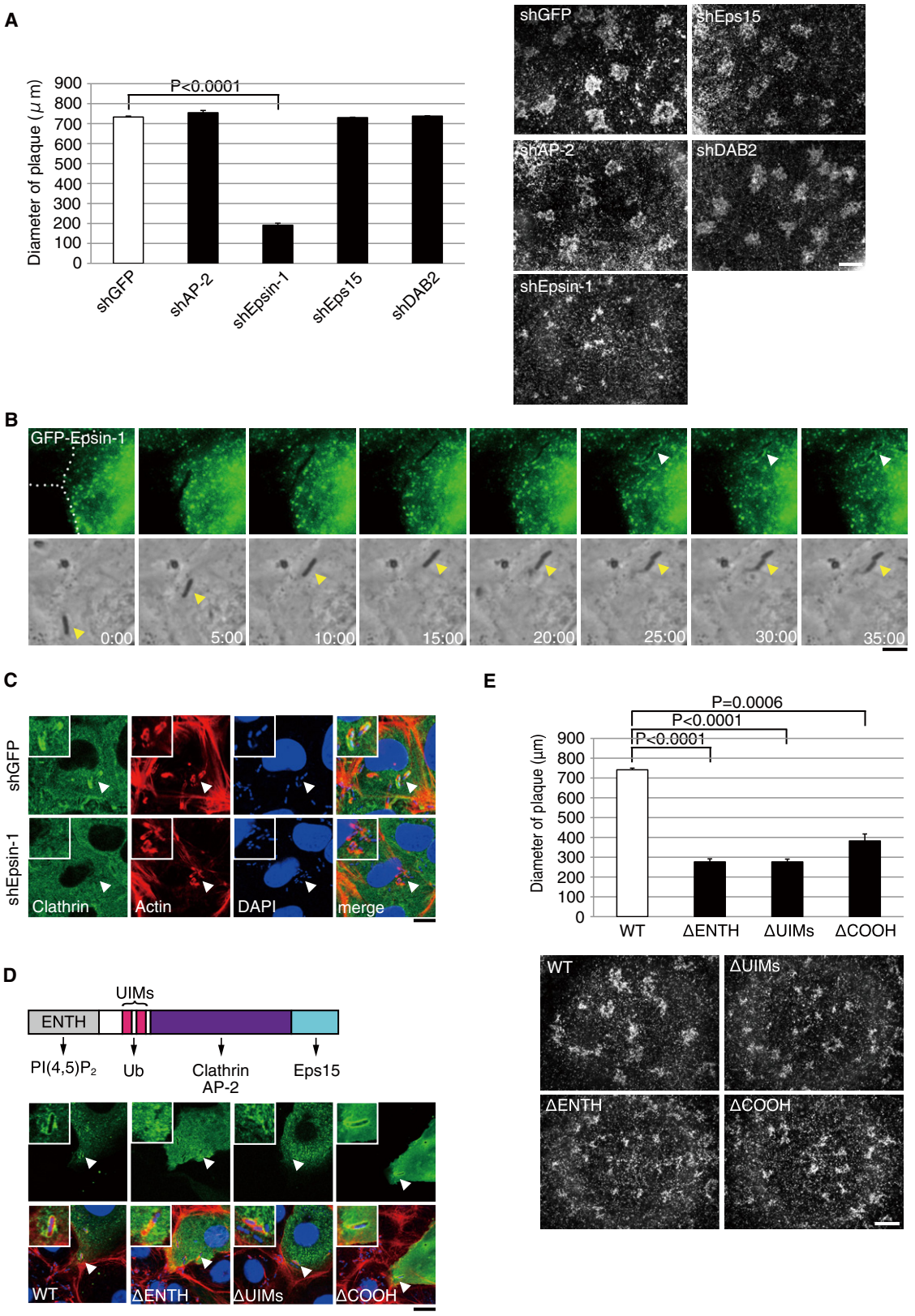

Figure 4. Epsin-1 Was Required to Recruit Clathrin to *Shigella*-Containing Pseudopodia

(A) MDCK cells stably expressing the indicated shRNA were infected with *Shigella*. After 2 days, plaque formation was examined. Scale bar, 500 μm. The diameter of the plaques was measured. Data are the means ± SEM (>15 plaques, n = 3). (See also Figure S4.)

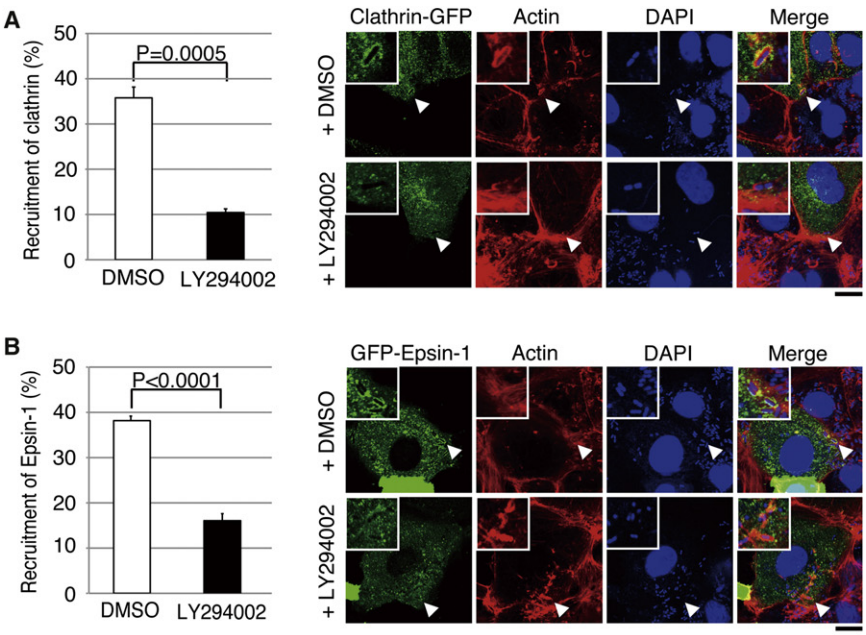

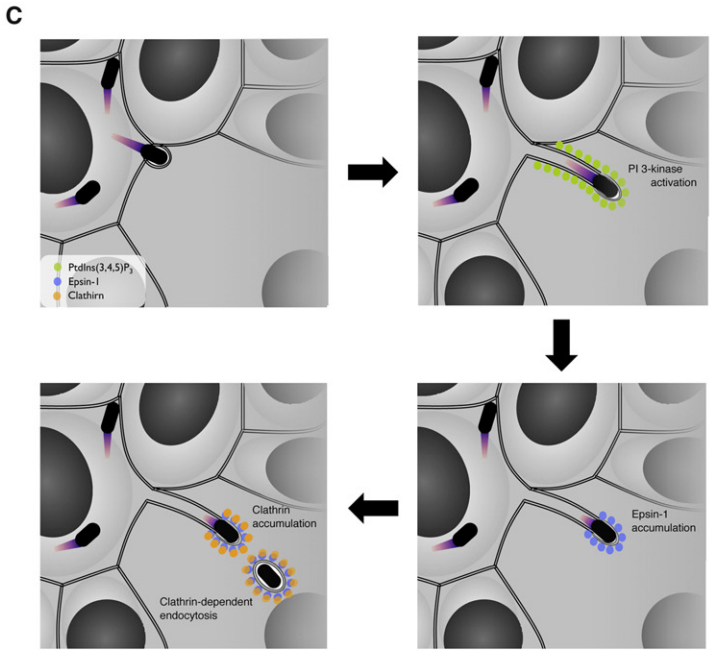

Figure 5. Effect of PI 3-Kinase Activity on the Localization of Clathrin-GFP and GFP-Epsin-1

(A and B) MK2 cells expressing clathrin-GFP (A) or GFP-Epsin-1 (B) were infected with *Shigella* for 2.5 hr in the presence or absence of LY294002 and then fixed. The cells were stained with rhodamine-phalloidin and DAPI. Scale bar, 20 μm. The population of clathrin-positive (A) or Epsin-1-positive (B) pseudopodia was quantified. Data are the means ± SEM (>50 pseudopodia, n = 3).

(C) Proposed model for *Shigella* cell-cell spreading. When *Shigella* move from one epithelial cell to neighboring epithelial cells, *Shigella*-containing pseudopodia target tricellular tight junctions. PI 3-kinase is activated upon formation of a *Shigella*-containing pseudopodium. PI 3-kinase activity is required to recruit Epsin-1 and clathrin to the plasma membrane where the bacteria-containing pseudopodium was engulfed. Finally, an elongating pseudopodium is fully engulfed by a neighboring cell and undergoes clathrin-dependent endocytosis.

expression had no effect on clathrin-mediated internalization of transferrin, EGF, or LDL, in which AP-2, Esp15, and Epsin-1 rapidly accumulate beneath the endocytosed plasma membrane (Keyel et al., 2006; Vanden Broeck and De Wolf, 2006). Therefore, the mechanisms underlying internalization of bacteria-containing pseudopodia and clathrin-dependent recycling of transferrin, EGF, and LDL appear to differ (Keyel et al., 2006). Additionally, studies are needed to characterize this noncanonical clathrin-mediated pathway, including the identification of cargo protein(s) that interacts with Epsin-1 during *Shigella* cell-cell spreading.

In summary, *Shigella* cell-cell movement frequently occurs at tTJs, where *Shigella*-containing pseudopodia are engulfed by neighboring cells via a noncanonical clathrin-dependent endocytic pathway.

EXPERIMENTAL PROCEDURES

Bacterial Strains

Shigella flexneri YSH6000 cells were used as the wild-type strain. *Shigella* were cultured overnight at 30°C in L broth, diluted 1:100 in brain-heart infusion (BHI) broth (Difco), and grown for 2 hr at 37°C. To visualize living bacteria, pUC-GFP or pBR322-DsRed was transformed into *Shigella*. GFP- or DsRed-expressing *Shigella* were cultured overnight at 30°C in Mueller Hinton broth supplemented with 5 μg × ml^{-1} trimethoprim, diluted 1:50 in BHI broth, and grown for 2 hr at 37°C. To create GFP-expressing wild-type EGD *L. monocytogenes*, pMV158-GFP was transformed into *Listeria*, which was cultured overnight at

(B) MK2 cells expressing GFP-Epsin-1 were infected with *Shigella*. Images were acquired at 1 min intervals after infection. The time after pseudopodium formation is indicated. White and yellow arrowheads indicate Epsin-1 accumulation or *Shigella*-containing pseudopodia, respectively. Scale bar, 5 μm. (See also Movie S4.)

(C) The recruitment of clathrin to the pseudopodium membrane was examined. MDCK cells stably expressing the indicated shRNA were infected with *Shigella* for 2.5 hr and then fixed. The cells were stained with an anti-clathrin heavy chain antibody, rhodamine-phalloidin, and DAPI. Scale bar, 20 μm. (See also Figure S4.)

(D) Schematic illustration of wild-type Epsin-1. MK2 cells expressing GFP-Epsin-1 (WT and deletion mutant) were infected with *Shigella* for 2.5 hr and then fixed. The cells were stained with rhodamine-phalloidin and DAPI. Scale bar, 20 μm. (See also Figure S4.)

(E) MDCK cells stably expressing the indicated construct were infected with *Shigella*. After 2 days, plaque formation was examined. Scale bar, 500 μm. The diameter of the plaques was measured. Data are the means ± SEM (>15 plaques, n = 3).

30°C in BHI broth supplemented with 2.5 μg × ml^{-1} tetracycline, diluted 1:25 in BHI broth, and grown for 2 hr at 37°C.

Time-Lapse Microscopy

MK2 cells (the shape of MK2 cells is thin, which made it feasible to monitor the fate of *Shigella*-containing pseudopodia) were grown on collagen-coated 35 mm glass-bottom dishes for 2 days and then infected with *Shigella* at a multiplicity of infection (moi) of 100 or *Listeria* at a moi of 1. The infection was initiated by centrifuging the plate at 700 g for 10 min. After 1 hr or 1.5 hr incubation at 37°C, the cells were washed three times with fresh medium without FCS and then cultured in fresh medium containing 10% FCS, 100 μg × ml^{-1} of gentamicin, and 60 μg × ml^{-1} of kanamycin to kill any extracellular bacteria. Live images of infected cells were captured with an AxioObserver Z.1 (Carl Zeiss) and analyzed with AxioVision 4.6 software (Carl Zeiss).

Electron Microscopy

MK2 cells were grown on collagen-coated coverslips for 2 days and infected with *Shigella* at an moi of 50, as described above. After 1 hr infection at 37°C, the cells were washed three times with fresh medium without FCS and then cultured in fresh medium containing 10% FCS, 100 μg × ml^{-1} of gentamicin and 60 μg × ml^{-1} of kanamycin. After incubating for 2.5 hr at 37°C, the cells were fixed using a conventional method (1.5% paraformaldehyde and 3% glutaraldehyde in 0.1 M phosphate buffer, pH 7.3, followed by an aqueous solution of 1% OsO_4) (Nishida et al., 2009). The fixed cells were embedded in Epon 812. Thin sections were cut and stained with uranyl acetate and lead citrate and then observed under a JEOL-1010 electron microscope (JEOL) at 80 kV.

Plaque Formation Assay

The intracellular dissemination of bacteria was evaluated using a plaque formation assay (Ogawa et al., 2003). The polarized MDCK cells are well suited to plaque formation assay for *Shigella* cell-cell movement. Stably expressed MDCK cells or knocked down MDCK cells were grown in 12-well plates and cultured for 2 days to a confluent monolayer. The cells were washed with Hank's balanced salt solution (HBSS) supplemented with 100 μM ethylene glycol-bis (β-amino-ethyl ether)-N,N,N′,N′-tetra-acetic acid (EGTA) and then infected with *Shigella* suspended in HBSS supplemented with 100 μM EGTA for 1 hr at 37°C. After the infection, the cells were washed three times with fresh medium without FCS, and then the medium was replaced with fresh medium containing 10% FCS, 100 μg × ml^{-1} of gentamicin, and 60 μg × ml^{-1} of kanamycin. The cells were cultured at 37°C for 2 days in the presence of 5% CO_2. The diameter of plaques was measured with a phase-contrast microscope equipped with a CCD camera using AxioObserver Z.1 and analyzed with AxioVision 4.6 software.

Intercellular Spreading

Caco-2 cells or MDCK cells were grown for 2 days on collagen-coated coverslips and infected with GFP-expressing *Shigella* at an moi of 10 or GFP-expressing *Listeria* at an moi of 1, as described above. After a 1 hr or 1.5 hr infection at 37°C, the cells were washed three times with fresh medium without FCS, and the medium was replaced with fresh medium containing 10% FCS, 100 μg × ml^{-1} of gentamicin, and 60 μg × ml^{-1} of kanamycin in the presence or absence of LY294002 (20 μM), wortmannin (20nM), PAO (0.2 μM), MβCD (10 mM), or EIPA (50 μM). After 8 hr incubation at 37°C, the cells were fixed with 4% paraformaldehyde in PBS, stained with rhodamine-phalloidin, and then analyzed with an LSM510 microscope (Carl Zeiss). The number of infected cells was determined by visual counting.

Giemsa Staining

Caco-2 cells were grown 2 days on collagen-coated coverslips and infected with *Shigella* at an moi of 50, as described above. After a 1 hr infection at 37°C, the cells were washed three times with fresh medium without FCS, and the medium was replaced with fresh medium containing 10% FCS, 100 μg × ml^{-1} gentamicin, and 60 μg × ml^{-1} kanamycin. After incubating for 2.5 hr at 37°C, the cells were fixed with methanol, stained with Giemsa's solution (Merck), and then examined using a phase-contrast microscope ECLIPSE E600 (Nikon).

Examining Proteins Associated with *Shigella*-Containing Pseudopodia

Caco-2 and MDCK cells were grown for 2 days on collagen-coated coverslips and infected with *Shigella* at an moi of 200, as described above. After infection for 1 hr at 37°C, the cells were washed three times with fresh medium without FCS, and the medium was replaced with fresh medium containing 10% FCS, 100 μg × ml^{-1} gentamicin, and 60 μg × ml^{-1} kanamycin. After incubating the samples for 2.5 hr at 37°C, cells were fixed with 4% paraformaldehyde in PBS. Fixed cells were quenched with 50 mM NH_4Cl in PBS, permeabilized with 0.2% Triton X-100 in PBS, and blocked with 2% BSA in TBS. After staining with the indicated antibodies, specimens were analyzed using a LMS510 microscope. MK2 cells expressing clathrin-GFP, Dynamin-2-GFP, and GFP-Epsin-1 were grown for 2 days on collagen-coated coverslips and infected with *Shigella* at an moi of 200 or 50, as described above. After infection for 1 hr at 37°C, cells were washed three times with fresh medium without FCS, and the medium was replaced with fresh medium containing 10% FCS, 100 μg × ml^{-1} gentamicin, and 60 μg × ml^{-1} kanamycin. After incubating the samples for 2.5 hr at 37°C, the cells were fixed with 4% paraformaldehyde in PBS, stained with rhodamine-phalloidin, and analyzed using an LSM510.

Quantification of *Shigella*-Containing Pseudopodia

Shigella-containing pseudopodia were counted on captured images with time-lapse movies.

Quantification of GFP-Epsin1 and Clathrin-GFP around *Shigella*-Containing Pseudopodia

The populations of MK2 cells with GFP-Epsin-1-positive or clathrin-GFP-positive pseudopodia and MDCK cells with clathrin-positive pseudopodia were counted using an LSM510 microscope.

Statistical Analysis

Statistical analyses were performed using the unpaired two-tailed Student's t test. Differences were considered significant when $p < 0.01$.

SUPPLEMENTAL INFORMATION

Supplemental Information includes four figures, Supplemental Experimental Procedures, Supplemental References, and four movies and can be found with this article online at doi:10.1016/j.chom.2012.03.001.

ACKNOWLEDGMENTS

We thank Mikio Furuse for his advice. We also thank the members of the Sasakawa laboratory for their advice. This work was supported by a Grant-in-Aid for Specially Promoted Research (23000012, C.S.); a Grant-in-Aid for Young Scientists (A) (23689027, M.K.); a Grant-in-Aid for Young Scientists (B) (23790471, M.O.); a Grant-in-Aid for Scientific Research (B) (23390102, H.M.); a Grant-in-Aid for Challenging Exploratory Research (23659220, H.M.); a Grant-in-Aid for Scientific Research on Priority Areas (18073003, C.S.); and Japan Initiative for Global Research Network on Infectious Diseases (C.S.). Part of this work was supported by grants from the Naito Foundation (H.M. and M.K.), the Waksman Foundation of Japan Inc. (M.O.), the Yakult Bio-Science Foundation (M.O.), the Yakult Central Institute (C. S.), the Hayashi Memorial Foundation for Female Natural Science (M.K.), and the Takeda Science Foundation (M.K.).

Received: October 18, 2011
Revised: January 7, 2012
Accepted: February 14, 2012
Published: April 18, 2012

REFERENCES

Chen, C., and Zhuang, X. (2008). Epsin 1 is a cargo-specific adaptor for the clathrin-mediated endocytosis of the influenza virus. Proc. Natl. Acad. Sci. USA *105*, 11790–11795.

Chen, H., Fre, S., Slepnev, V.I., Capua, M.R., Takei, K., Butler, M.H., Di Fiore, P.P., and De Camilli, P. (1998). Epsin is an EH-domain-binding protein implicated in clathrin-mediated endocytosis. Nature *394*, 793–797.

Collins, A., Warrington, A., Taylor, K.A., and Svitkina, T. (2011). Structural organization of the actin cytoskeleton at sites of clathrin-mediated endocytosis. Curr. Biol. *21*, 1167–1175.

Conibear, E. (2010). Converging views of endocytosis in yeast and mammals. Curr. Opin. Cell Biol. *22*, 513–518.

Conner, S.D., Schröter, T., and Schmid, S.L. (2003). AAK1-mediated micro2 phosphorylation is stimulated by assembled clathrin. Traffic *4*, 885–890.

Cossart, P., and Sansonetti, P.J. (2004). Bacterial invasion: the paradigms of enteroinvasive pathogens. Science *304*, 242–248.

Cureton, D.K., Massol, R.H., Whelan, S.P., and Kirchhausen, T. (2010). The length of vesicular stomatitis virus particles dictates a need for actin assembly during clathrin-dependent endocytosis. PLoS Pathog. *6*, e1001127.

de Beco, S., Gueudry, C., Amblard, F., and Coscoy, S. (2009). Endocytosis is required for E-cadherin redistribution at mature adherens junctions. Proc. Natl. Acad. Sci. USA *106*, 7010–7015.

Drake, M.T., Downs, M.A., and Traub, L.M. (2000). Epsin binds to clathrin by associating directly with the clathrin-terminal domain. Evidence for cooperative binding through two discrete sites. J. Biol. Chem. *275*, 6479–6489.

Edelblum, K.L., and Turner, J.R. (2009). The tight junction in inflammatory disease: communication breakdown. Curr. Opin. Pharmacol. *9*, 715–720.

Ferguson, S.M., Raimondi, A., Paradise, S., Shen, H., Mesaki, K., Ferguson, A., Destaing, O., Ko, G., Takasaki, J., Cremona, O., et al. (2009). Coordinated actions of actin and BAR proteins upstream of dynamin at endocytic clathrin-coated pits. Dev. Cell *17*, 811–822.

Ford, M.G., Mills, I.G., Peter, B.J., Vallis, Y., Praefcke, G.J., Evans, P.R., and McMahon, H.T. (2002). Curvature of clathrin-coated pits driven by epsin. Nature *419*, 361–366.

Ikenouchi, J., Furuse, M., Furuse, K., Sasaki, H., Tsukita, S., and Tsukita, S. (2005). Tricellulin constitutes a novel barrier at tricellular contacts of epithelial cells. J. Cell Biol. *171*, 939–945.

Ikenouchi, J., Sasaki, H., Tsukita, S., Furuse, M., and Tsukita, S. (2008). Loss of occludin affects tricellular localization of tricellulin. Mol. Biol. Cell *19*, 4687–4693.

Itoh, T., Koshiba, S., Kigawa, T., Kikuchi, A., Yokoyama, S., and Takenawa, T. (2001). Role of the ENTH domain in phosphatidylinositol-4,5-bisphosphate binding and endocytosis. Science *291*, 1047–1051.

Ivanov, A.I., Nusrat, A., and Parkos, C.A. (2005). Endocytosis of the apical junctional complex: mechanisms and possible roles in regulation of epithelial barriers. Bioessays *27*, 356–365.

Keyel, P.A., Mishra, S.K., Roth, R., Heuser, J.E., Watkins, S.C., and Traub, L.M. (2006). A single common portal for clathrin-mediated endocytosis of distinct cargo governed by cargo-selective adaptors. Mol. Biol. Cell *17*, 4300–4317.

Koch, S., and Nusrat, A. (2009). Dynamic regulation of epithelial cell fate and barrier function by intercellular junctions. Ann. N Y Acad. Sci. *1165*, 220–227.

Krug, S.M., Amasheh, S., Richter, J.F., Milatz, S., Günzel, D., Westphal, J.K., Huber, O., Schulzke, J.D., and Fromm, M. (2009). Tricellulin forms a barrier to macromolecules in tricellular tight junctions without affecting ion permeability. Mol. Biol. Cell *20*, 3713–3724.

Le, T.L., Yap, A.S., and Stow, J.L. (1999). Recycling of E-cadherin: a potential mechanism for regulating cadherin dynamics. J. Cell Biol. *146*, 219–232.

Lindmo, K., and Stenmark, H. (2006). Regulation of membrane traffic by phosphoinositide 3-kinases. J. Cell Sci. *119*, 605–614.

Madara, J.L. (1990). Maintenance of the macromolecular barrier at cell extrusion sites in intestinal epithelium: physiological rearrangement of tight junctions. J. Membr. Biol. *116*, 177–184.

McMahon, H.T., and Boucrot, E. (2011). Molecular mechanism and physiological functions of clathrin-mediated endocytosis. Nat. Rev. Mol. Cell Biol. *12*, 517–533.

Merrifield, C.J., Perrais, D., and Zenisek, D. (2005). Coupling between clathrin-coated-pit invagination, cortactin recruitment, and membrane scission observed in live cells. Cell *121*, 593–606.

Motley, A., Bright, N.A., Seaman, M.N., and Robinson, M.S. (2003). Clathrin-mediated endocytosis in AP-2-depleted cells. J. Cell Biol. *162*, 909–918.

Nishida, Y., Arakawa, S., Fujitani, K., Yamaguchi, H., Mizuta, T., Kanaseki, T., Komatsu, M., Otsu, K., Tsujimoto, Y., and Shimizu, S. (2009). Discovery of Atg5/Atg7-independent alternative macroautophagy. Nature *461*, 654–658.

Ogawa, M., Suzuki, T., Tatsuno, I., Abe, H., and Sasakawa, C. (2003). IcsB, secreted via the type III secretion system, is chaperoned by IpgA and required at the post-invasion stage of Shigella pathogenicity. Mol. Microbiol. *48*, 913–931.

Ogawa, M., Handa, Y., Ashida, H., Suzuki, M., and Sasakawa, C. (2008). The versatility of Shigella effectors. Nat. Rev. Microbiol. *6*, 11–16.

Otani, T., Ichii, T., Aono, S., and Takeichi, M. (2006). Cdc42 GEF Tuba regulates the junctional configuration of simple epithelial cells. J. Cell Biol. *175*, 135–146.

Pentecost, M., Otto, G., Theriot, J.A., and Amieva, M.R. (2006). Listeria monocytogenes invades the epithelial junctions at sites of cell extrusion. PLoS Pathog. *2*, e3.

Pentecost, M., Kumaran, J., Ghosh, P., and Amieva, M.R. (2010). Listeria monocytogenes internalin B activates junctional endocytosis to accelerate intestinal invasion. PLoS Pathog. *6*, e1000900.

Pizarro-Cerdá, J., Bonazzi, M., and Cossart, P. (2010). Clathrin-mediated endocytosis: what works for small, also works for big. Bioessays *32*, 496–504.

Polo, S., Sigismund, S., Faretta, M., Guidi, M., Capua, M.R., Bossi, G., Chen, H., De Camilli, P., and Di Fiore, P.P. (2002). A single motif responsible for ubiquitin recognition and monoubiquitination in endocytic proteins. Nature *416*, 451–455.

Rajabian, T., Gavicherla, B., Heisig, M., Müller-Altrock, S., Goebel, W., Gray-Owen, S.D., and Ireton, K. (2009). The bacterial virulence factor InlC perturbs apical cell junctions and promotes cell-to-cell spread of Listeria. Nat. Cell Biol. *11*, 1212–1218.

Rathman, M., de Lanerolle, P., Ohayon, H., Gounon, P., and Sansonetti, P. (2000). Myosin light chain kinase plays an essential role in S. flexneri dissemination. J. Cell Sci. *113*, 3375–3386.

Rong, S.B., Hu, Y., Enyedy, I., Powis, G., Meuillet, E.J., Wu, X., Wang, R., Wang, S., and Kozikowski, A.P. (2001). Molecular modeling studies of the Akt PH domain and its interaction with phosphoinositides. J. Med. Chem. *44*, 898–908.

Sansonetti, P.J., Mounier, J., Prévost, M.C., and Mège, R.M. (1994). Cadherin expression is required for the spread of Shigella flexneri between epithelial cells. Cell *76*, 829–839.

Shen, L., Weber, C.R., and Turner, J.R. (2008). The tight junction protein complex undergoes rapid and continuous molecular remodeling at steady state. J. Cell Biol. *181*, 683–695.

Shen, A., Zhou, D., Shen, Q., Liu, H.O., Sun, L., Liu, Y., Chen, J., Yang, J., Ji, Y., and Cheng, C. (2009). The expression of tumor necrosis factor-alpha (TNF-alpha) by the intrathecal injection of lipopolysaccharide in the rat spinal cord. Neurochem. Res. *34*, 333–341.

Shen, L., Weber, C.R., Raleigh, D.R., Yu, D., and Turner, J.R. (2011). Tight junction pore and leak pathways: a dynamic duo. Annu. Rev. Physiol. *73*, 283–309.

Shih, S.C., Katzmann, D.J., Schnell, J.D., Sutanto, M., Emr, S.D., and Hicke, L. (2002). Epsins and Vps27p/Hrs contain ubiquitin-binding domains that function in receptor endocytosis. Nat. Cell Biol. *4*, 389–393.

Steed, E., Balda, M.S., and Matter, K. (2010). Dynamics and functions of tight junctions. Trends Cell Biol. *20*, 142–149.

Tilney, L.G., and Portnoy, D.A. (1989). Actin filaments and the growth, movement, and spread of the intracellular bacterial parasite, Listeria monocytogenes. J. Cell Biol. *109*, 1597–1608.

Tran Van Nhieu, G., Clair, C., Bruzzone, R., Mesnil, M., Sansonetti, P., and Combettes, L. (2003). Connexin-dependent inter-cellular communication increases invasion and dissemination of Shigella in epithelial cells. Nat. Cell Biol. *5*, 720–726.

Troyanovsky, R.B., Sokolov, E.P., and Troyanovsky, S.M. (2006). Endocytosis of cadherin from intracellular junctions is the driving force for cadherin adhesive dimer disassembly. Mol. Biol. Cell *17*, 3484–3493.

Utech, M., Mennigen, R., and Bruewer, M. (2010). Endocytosis and recycling of tight junction proteins in inflammation. J. Biomed. Biotechnol. *2010*, 484987.

Vanden Broeck, D., and De Wolf, M.J. (2006). Selective blocking of clathrin-mediated endocytosis by RNA interference: epsin as target protein. Biotechniques *41*, 475–484.

Veiga, E., and Cossart, P. (2005). Listeria hijacks the clathrin-dependent endocytic machinery to invade mammalian cells. Nat. Cell Biol. *7*, 894–900.

Vieira, O.V., Botelho, R.J., Rameh, L., Brachmann, S.M., Matsuo, T., Davidson, H.W., Schreiber, A., Backer, J.M., Cantley, L.C., and Grinstein, S. (2001). Distinct roles of class I and class III phosphatidylinositol 3-kinases in phagosome formation and maturation. J. Cell Biol. *155*, 19–25.

Westphal, J.K., Dörfel, M.J., Krug, S.M., Cording, J.D., Piontek, J., Blasig, I.E., Tauber, R., Fromm, M., and Huber, O. (2010). Tricellulin forms homomeric and heteromeric tight junctional complexes. Cell. Mol. Life Sci. *67*, 2057–2068.